Spatial quantization of exciton-polariton condensates in optically induced traps

Ekaterina Aladinskaia,[1] Roman Cherbunin,[1,*] Evgeny Sedov,[2,3,1,4] Alexey Liubomirov,[1] Kirill Kavokin,[1] Evgeny Khramtsov,[1] Mikhail Petrov,[1] P. G. Savvidis,[2,3,5,6] and Alexey Kavokin[2,3,1,7]

[1]*Spin Optics Laboratory, St. Petersburg State University, Ulyanovskaya 1, St. Petersburg 198504, Russia*

[2]*Key Laboratory for Quantum Materials of Zhejiang Province, School of Science, Westlake University, 18 Shilongshan Road, Hangzhou 310024, Zhejiang, China*

[3]*Institute of Natural Sciences, Westlake Institute for Advanced Study, 18 Shilongshan Road, Hangzhou, Zhejiang Province 310024, China*

[4]*Vladimir State University named after A. G. and N. G. Stoletovs, Gorky Street 87, Vladimir 600000, Russia*

[5]*FORTH-IESL, P.O. Box 1527, 71110 Heraklion, Crete, Greece*

[6]*Department of Materials Science and Technology, University of Crete, P.O. Box 2208, 71003 Heraklion, Crete, Greece*

[7]*Moscow Institute of Physics and Technology, Institutskiy Pereulok, 9, Dolgoprudnyi, Moscow Region 141701, Russia*

(Received 2 November 2022; accepted 20 December 2022; published 11 January 2023)

We study the formation of exciton-polariton condensates in potlike traps created by optical pumping in a planar microcavity with embedded quantum wells. The trap is formed by a repulsive reservoir of incoherent excitons excited by a ring-shaped nonresonant laser beam. Polariton condensates confined in a trapping potential are subject to spatial confinement leading to energy quantization. We reveal experimentally the discrete spectrum of polariton eigenstates in an optical trap that can be characterized by a pair of quantum numbers, azimuthal and radial quantum numbers, that correspond to the number of nodes of a condensate wave function in the corresponding directions. The occupation numbers of the eigenstates of a polariton condensate are determined by the overlap integral of the condensate wave function and the exciton reservoir spatial density distribution. The nonresonant pumping scheme enables engineering the shape and size of the trap, that allows to selectively excite specific superpositions of the eigenstates of a polariton condensate in each experiment. We demonstrate both single- and multiple-mode polariton lasing in an optical trap.

DOI: 10.1103/PhysRevB.107.045302

I. INTRODUCTION

Exciton cavity polaritons, hereafter referred to as simply polaritons, are light-matter quasiparticles formed due to the strong coupling of photons in an optical microcavity and excitons in quantum wells [1]. Being composite bosons, the polaritons are able to undergo stimulated transitions to the macroscopically occupied coherent quantum state of a dynamical Bose-Einstein condensate [2] analogous to one in an ultracold atomic system [3]. Semiconductor microcavities can be considered as two-dimensional (2D) quantum systems since the polaritons are confined in the structure growth direction. It is well known [4,5], that bosonic condensation in ideal infinite 2D systems at finite temperatures is not possible. Nevertheless, in real systems this limitation is usually circumvented by the presence of an effective confining potential for polaritons in the microcavity plane that enables quasicondensation or the formation of bosonic condensates having a discrete energy spectrum. The confinement can be provided by a lateral potential [2,6], provided by the edges of a finite-size sample [7–15], by local modulations of the cavity layer thickness (so-called *mesas*) [16,17], or artificially generated by an external impact [18–22]. The potentials created at the stage of growth of the sample have the advantage of stability in their optical and energy properties, which, however, cannot be easily tuned. Micropillars are a striking representative of structures with this type of confining potential. In Refs. [10–15] a sample representing a high-quality planar $5\lambda/2$ AlGaAs distributed Bragg reflector microcavity with a set of etched cylindrical micropillars of different diameters is studied. The variation of the cavity layer width leads to different exciton-photon energy detunings in different micropillars. By selecting from an ensemble of available micropillars, one can choose specific localization conditions for the polaritons. However, fine tuning of the properties of the localizing potential still remains impossible. The effect of the size of the micropillar on the eigenstates of the confining potential has been discussed in Refs. [14,15].

Alternatively, a trap for polaritons can be created by applying a local stress to the microcavity sample by pressing on it with a thin pin from the backside [18,19]. Polaritons nonresonantly excited by a laser pump at the side of the trapping potential tend to reach its minimum and join the condensate state. In this geometry, the spatial separation of the polariton condensate and the excitation spot proves that the coherence of the condensate is not inherited from the excitation radiation. The depth of the strain-induced trap is tunable, and it depends on the applied pressure. However, the range of the tuning is limited by the thickness and mechanical rigidity of the sample.

*r.cherbunin@spbu.ru

Another option for trapping polaritons, which gives much more flexibility, is by means of optically induced traps [21,22]. Nonresonant optical pumping creates a reservoir of incoherent excitons in a microcavity plane. Due to the repulsive nature of polariton-exciton interactions, the exciton reservoir, which is mostly localized under the pump spot, acts as a potential barrier for polaritons. We are aware of multiple publications on the properties of polariton condensates in optical traps of different shapes [22–26] including a ring shape created using axicons [22], and a multiple-spot shape [24,25]. One of the problems of interest is the formation of azimuthal polariton currents in exciton-polariton condensates localized in optical traps [25,26].

The formation of different modes of trapped polariton condensates was studied previously in optically induced annular traps by Berger *et al.* [27]. It was found that with an increase of the trap's size and the pumping power, exciton-polariton condensates with different orbital angular momenta (OAM), which correspond to clockwise and anticlockwise polariton currents, were formed. The state with a nonzero OAM was described as a vortex in a localized polariton superfluid. The existence of the polariton mode with definite nonzero OAM was explained in terms of the interplay between the vortex core size and the trap size.

In this paper, we study the problem of shaping and the selective excitation of exciton-polariton condensates in a potlike optical trap induced by a nonresonant annular laser pump in a planar microcavity. We observe experimentally both the ground and the excited states of a polariton condensate in a trap. Additionally, we perform real-space spectral imaging of the condensate emission and observe that different condensate modes correspond to single-particle quantum levels. While the ground state has zero OAM, the excited states can carry nonzero OAM, as it happens in atoms. The tunability of the shape of the trap enables us to study the effect of the trap size on the occupation of the condensate eigenstates.

II. EXPERIMENTS

We study a planar $Al_{0.15}Ga_{0.85}As$ microcavity of width $5\lambda/2$ with 12 embedded GaAs quantum wells and placed between two high-quality (with a Q factor exceeding 10^4) distributed Bragg reflectors (DBRs). The top (bottom) DBR consists of 45 (50) pairs of $AlAs/Al_{0.3}Ga_{0.7}As$.

We use a Millenia-eV pumped Tsunami Ti:sapphire pulsed picosecond laser tuned to a wavelength of 751 nm to excite a polariton condensate in the sample. The laser beam had passed through an acousto-optical modulator (AOM) to control the incident pump power. After AOM, the diffracted beam was directed to a micromirror spatial light modulator (SLM) (Texas Instruments model DLP9000, pixel size = 7.56 μm). The output pattern on the SLM defines the spatial profile of the pumping beam and, consequently, the shape of the trap. After reflection from SLM, the light beam was focused on the sample surface with a magnification factor of 4:125 by using an $F = 125$ mm converging lens followed by a 50× Mitutoyo microscope objective (focal length of $F = 4$ mm). The photoluminescence (PL) of the condensate was collected by the same objective in a backscattering geometry, filtered with a long-pass spectral filter FELH800, and then detected by a Meade DSI IV CMOS camera or by a 0.5-m Acton HRS-500 imaging spectrometer with a PIXIS-256 CCD camera. Each spectrum was obtained by accumulating 10^8 independent condensates.

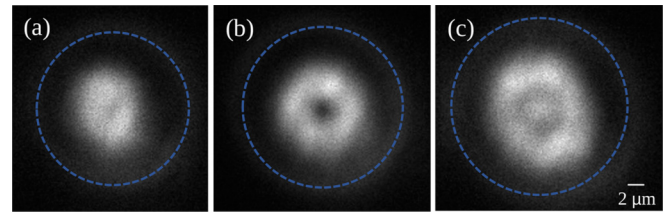

FIG. 1. Photoluminescence of the polariton condensates excited in potlike traps of different widths. The radii of the ring-shaped pump profile are (a) $R = 9$ μm, (b) $R = 9.4$ μm, and (c) $R = 10.4$ μm. The blue dashed circle shows the location of the optically induced trap.

In the experiment, we excite polaritons by a ring-shaped optical pump. The radius of the ring, R, is changed in the range 9–11 μm while the width of the ring, d, is always equal to a quarter of R ($d = 2$–2.5 μm). At a pumping power exceeding the polariton-lasing threshold ($P_{th} = 2.4$ mW for the trap with $R = 9$ μm, $P_{th} = 2.7$ mW for a trap with $R = 9.4$ μm, and $P_{th} = 3.3$ mW for a trap with $R = 10.4$ μm), the polaritons form a condensate inside the pump-induced optical trap. Herewith, the shape of the condensate considerably depends on the size of the trap. Figure 1 shows the polariton condensates formed in optical ring traps of different radii. In a trap of radius $R = 9$ μm [Fig. 1(a)] the polariton condensate occupies a bell-shaped state in the center of the trap. Once the radius increases to 10 μm [Fig. 1(b)], the condensate shape is changed into an annulus with a density dip in the center of the trap. A further increase in the radius to $R = 10.4$ μm [Fig. 1(c)] results in the formation of a condensate with a bell-shaped spot surrounded by an annulus ring centered in the trap.

To further understand the formation of the polariton condensates in the trap, we have performed real-space measurements of PL of a condensate emerging in a trap of $R = 9.4$ μm at different pumping powers. To this end, the condensate PL was focused on the slit of the spectrometer. Figure 2 shows the distribution of the condensate PL spectrum along the cross section of the trap. At the lowest pump power [Fig. 2(a)], a single-energy condensate is formed. The two symmetric spots on the tomography image showing the real space and energy distribution of the polaritons certify the symmetric ring shape of the condensate. Once the pumping power is increased, the ring-shaped state is supplemented with an additional state localized in the center of the trap which is red detuned in energy [Fig. 2(b)]. A further increase in pump power leads to the emergence of a triple-mode polariton condensate [Fig. 2(c)]. It worth mentioning that the results of real-space and spectrally resolved tomography measurements shown in Figs. 1 and 2, show the accumulated PL signals from multiple pumping pulses, so that we are unable to conclude if the polariton condensates of different energies emerged simultaneously or consecutively after different excitation pulses.

The energy distribution of a polariton condensate in a trap integrated over the cross section is shown in Fig. 3. To distinguish between different modes in the measured spec-

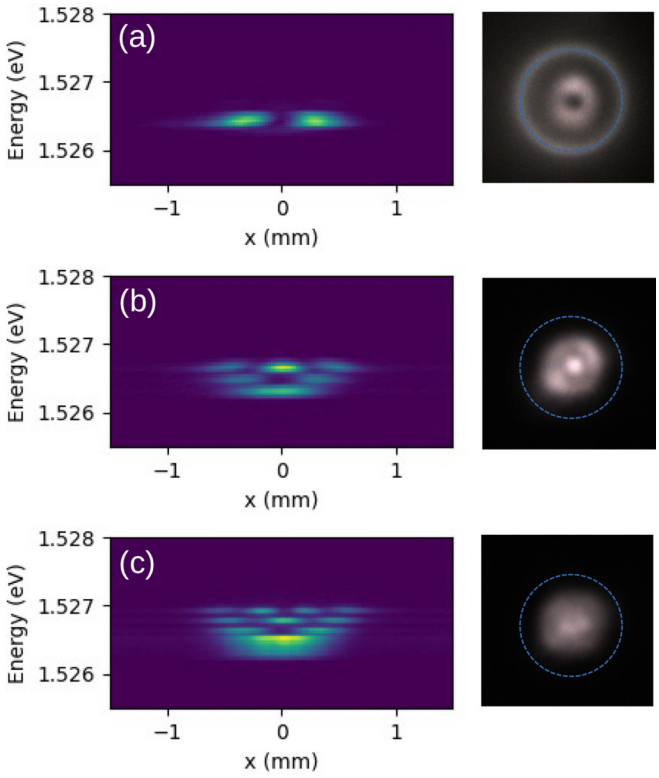

FIG. 2. Left side: Photoluminescence (PL) distribution intensity of the polariton condensate in an optical trap of radius $R = 9.8$ μm as a function of energy and real-space coordinate at different pumping powers. Right side: The corresponding real-space images. (a) $P = 1.2P_{\text{th}}$, (b) $P = 1.5P_{\text{th}}$, and (c) $P = 2.3P_{\text{th}}$. The blue dashed circle shows the location of the optically induced trap.

trum, we fit them by Gaussian functions with a fixed half width at half maximum (HWHM) equal to 65 μeV. As one can see by comparing traps of different widths, various numbers of modes of the trap can be occupied depending on the width of the trap and on the pumping power. In the smallest considered trap of $R = 9$ μm [Fig. 3(a)], the two condensate modes occur. At a weak pumping power ($P = 1.1P_{\text{th}}$), the lower mode (blue curve), which, in fact, is the ground eigenmode of the trap, dominates the upper (first excited) mode. With increasing pumping power, the contribution of the upper mode to the condensate PL increases and it becomes comparable to the one of the ground mode ($P = 1.5P_{\text{th}}$). For a wider trap of $R = 9.4$ μm [Fig. 3(b)], a single first-excited mode is replaced by three modes of almost equal intensities flaring up with an increase of pumping power. In the widest trap of $R = 10.4$ μm [Fig. 3(c)], two and four modes are occupied simultaneously at pumping powers of $P = 1.1P_{\text{th}}$ and $P = 1.4P_{\text{th}}$, respectively.

The spectral tomography of the condensate PL is an efficient method for analyzing its mode composition. It can be performed by measuring the spectrum of each pixel in the image by scanning the image of the condensate emission through the slit. All these spectra are collected into a single three-dimensional (3D) array: the pixel intensity as a function of x, y, and energy. A slice of this array at one fixed energy represents the image of the condensate wave function at a given energy [28]. The result of the real-space spectral tomography of the condensate in a trap with $R = 10.4$ μm and pumping power $P = 1.6P_{\text{th}}$ is shown in Figs. 4(a)–4(d). We reveal four polariton condensate states split in energy and possessing different spatial distributions in the trap. The shapes of the modes include a bell-like, single ring, i.e., a single ring with a spot in its center or a double concentric ring shape, respectively.

For the chosen trapping conditions, all four modes emit simultaneously. However, a reduction in the radius or the pumping power leads to a change in the set of emitting eigenmodes. The normalized intensity of different modes of the condensate as a function of the pumping power measured for different radii of the trap is shown in Fig. 5. In the trap of the smallest radius [Fig. 5(a)], only the two lowest condensate modes occur for the considered pumping-power range. The lowest mode is the most pronounced at a pumping power not exceeding $P \sim 1.4P_{\text{th}}$. With a further increase of P, the second mode starts dominating, herewith the intensities of both modes are comparable.

The most pronounced mode in the wider trap [Fig. 5(b)] is the second (ring-shaped) mode, namely one which carries a nonzero OAM. At a small pumping power, it remains the only emitting mode. At a pumping power approximately in the middle of the studied range, the first (ground) and the third modes emerge. Their intensities approach the intensity of the second mode with an increase of pumping power.

In a trap of radius $R = 10.4$ μm [Fig. 5(c)], the second and third modes prevail. At the small pumping power, the second mode is stronger in intensity. With increasing power, the modes swap. The first and fourth modes, which do not manifest themselves under weak pumping, appear with increasing pumping power.

While the appearance of a set of polariton modes in a trap is expected, in general, we observe that for traps of some specific radii only the second (ring-shaped) mode is populated. In order to clarify which process is responsible for the stabilization of the ring-shaped condensates, we consider a single polariton quantized in an infinite cylindrical potential that exponentially depends on the radial coordinate. This simplest model contains only two fitting parameters, namely, the polariton mass and the exciton diffusion length defining the shape of the potential. It predicts surprisingly well the shapes of polariton modes observed in the experiment, as we show below.

III. POLARITON EIGENMODES OF A POTLIKE POTENTIAL TRAP

While steady state solutions for a polariton condensate are usually modeled with the generalized Gross-Pitaevskii equation, in order to find out which mode(s) are to be occupied by the condensate in a trap, one should rather analyze a linear Schrödinger equation for a single exciton polariton. This is because below the condensation threshold all existing single polariton modes may be occupied by some nonzero probability, while the time-averaged occupation number of any mode is much less than 1, which is why polariton-polariton interactions are not important. Eventually, the condensate will be formed in a mode (linear combination of single-polariton modes) that is characterized by the lowest threshold

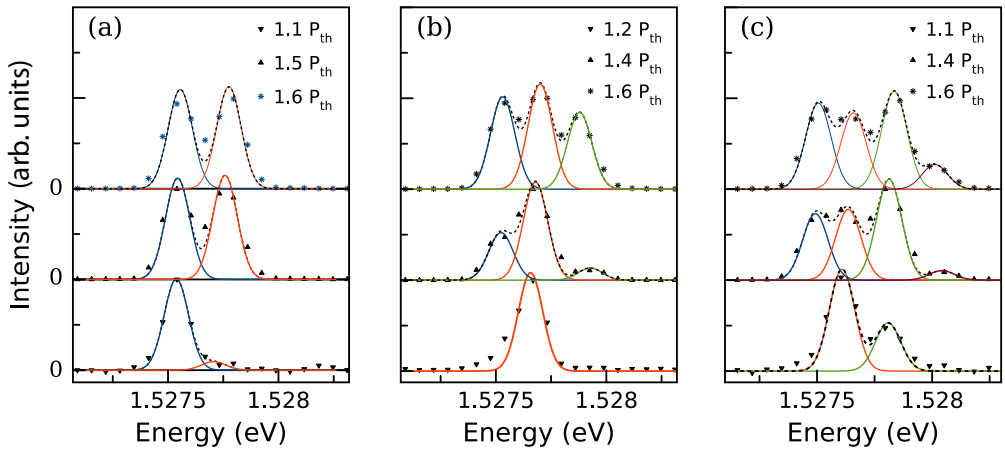

FIG. 3. Energy distribution of the intensity of the modes of the polariton condensate in traps of different radii at different pumping powers. The radius of the trap is (a) $R = 9$ μm, (b) $R = 9.4$ μm, and (c) $R = 10.4$ μm. The pumping power is indicated in the panels. Black markers show the results of the measurements, and colored curves show the fit to the spectra by the Gaussian functions with a fixed HWHM equal to 65 μeV. The number of condensate modes [from first (ground) to fourth] is indicated by the color of the curve (blue, red, green, and brown, respectively).

to stimulated scattering. If radiative lifetimes of polaritons in all modes of the trap are roughly equal, the condensate will be formed in a linear combination of modes that has the strongest overlap with the exciton reservoir. The largest overlap means the lowest threshold to polariton lasing in this case. It is important to note that the condensate as a whole entity is characterized by a much higher effective mass than a single polariton. The energy spectrum of excited states of an already formed condensate may be studied following the Bogoliubov–de Gennes approach based on the linearization of the Gross-Pitaevskii equation. This spectrum would also be discrete in a trap. Its study is beyond the scope of the present work.

Now, to evaluate the shape of a single-particle wave function $\Psi(\mathbf{r})$, we solve the Schrödinger equation for a single polariton localized in a potential trap,

$$-\nabla^2\Psi + U(\mathbf{r})\Psi = E\Psi, \tag{1}$$

where the first and second terms on the left-hand side of the equation are responsible for the kinetic and potential energy, and $U(\mathbf{r})$ is the trapping potential for polaritons provided by the repulsive reservoir of optically induced incoherent excitons, $U(\mathbf{r}) \propto n_{\mathrm{exc}}(\mathbf{r})$. The density distribution of a reservoir in a linear regime follows the shape of the pump spot.

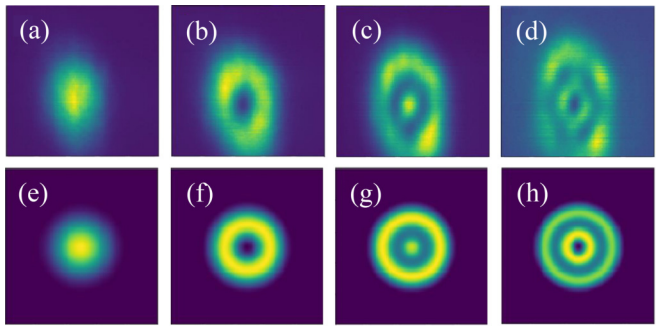

FIG. 4. Experimentally observed polariton modes at energies $E_1 = 1.5275$ eV, $E_2 = 1.5277$ eV, $E_3 = 1.5279$ eV, and $E_4 = 1.5281$ eV (a)–(d) and simulated (e)–(h) lowest four polariton condensate eigenstates of a trap induced by a ring-shaped optical pump with a radius of $R = 10.4$ μm at a power of $P = 1.6P_{\mathrm{th}}$.

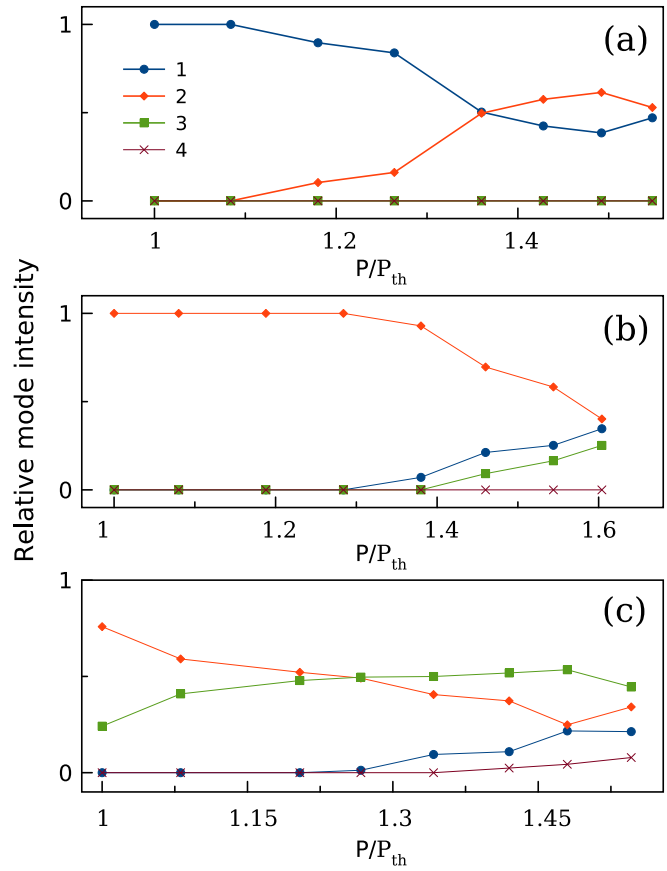

FIG. 5. Dependence of the relative intensity of the condensate modes vs pumping power measured for traps with different radii: (a) $R = 9$ μm, (b) $R = 9.4$ μm, and (c) $R = 10.4$ μm.

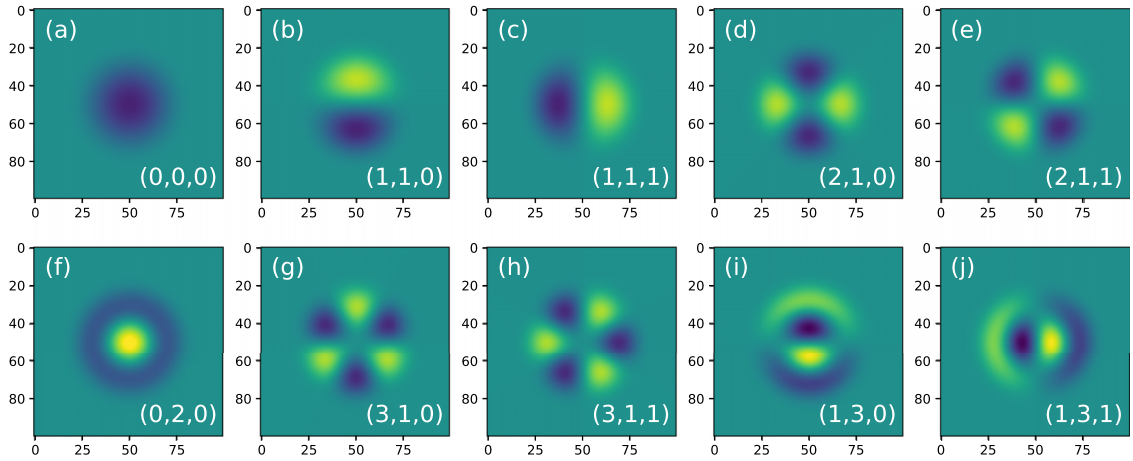

FIG. 6. Wave functions of the eigenstates of the potential trap $U(\mathbf{r})$ obtained from Eq. (1) at $w = 0.1R$. The set of quantum numbers (n, l, m) characterizing eigenstates is given in the right lower corner of each panel.

To describe the polariton eigenstates confined in the trap, we assume the exponential dependence of the reservoir density on the distance from the trap, $n_{\text{exc}}(\mathbf{r}) \propto \exp[-(R-r)/w]$, where R is the radius of the trap and w is the diffusion length of excitons.

Figure 6 shows the wave functions $\Psi(\mathbf{r})$ of the ten lowest eigenstates of the trap $U(\mathbf{r})$ obtained from Eq. (1). They are quite similar to Laguerre-Gaussian modes of light and can be quantified with the same set of quantum numbers (n, l, m), which denote the number of nodes in the azimuth (n) and radial (l) direction as well as the spatial orientation of the mode (m). The number of eigenstates in the trap depends on its height. The eigenstates shown in Figs. 6(a) and 6(f) reproduce qualitatively the experimentally observed states in Figs. 4(a) and 4(c), respectively. The quantum number m does not affect the eigenenergy of the trapped states. This enables any steady-state linear superposition of the eigenmodes, which differ in m only. For example, the superposition of the eigenmodes Ψ_{110} and Ψ_{111} yields the condensate state shown in Fig. 4(b), while the superposition of the eigenmodes Ψ_{130}, Ψ_{131}, Ψ_{310}, and Ψ_{311} yields the condensate state shown in Fig. 4(d).

As it was already mentioned, we assume that the condensate will be formed in a linear combination of eigenfunctions of the trap characterized by the largest overlap with the reservoir. For a given mode j characterized by the wave function Ψ_j, the overlap integral is given by

$$I_j = \int |\Psi_j(\mathbf{r})|^2 n_{\text{exc}}(\mathbf{r}) d\mathbf{r}. \tag{2}$$

The overlap integral as a function of the normalized exciton diffusion length w/R for different condensate states is shown in Fig. 7. If the diffusion length is much less than the radius of the trap, the overlap integrals for all eigenmodes of the condensate tend to zero. Conversely, if w considerably exceeds R, the overlap integrals tend to their maximal value. In the intermediate case corresponding to physically reasonable conditions where w and R are of the same order, the overlap integrals for different modes significantly differ from each other. The integrals increase with increasing ratio w/R. Herewith, as one can see, the higher in energy eigenstates are characterized by larger overlap integrals, which means a stronger gain from the pump. This clarifies the reason why the polariton condensate tends to occupy the highest excited states allowed by the trapping conditions and the pumping regime. The inset in Fig. 7 shows schematically the wave functions of the two lowest states in a potlike trap. This scheme enables us to visualize the overlap of the exciton reservoir with the polariton condensate wave functions in the trap.

IV. CONCLUSION

We have studied the formation of exciton-polariton condensates in potlike traps induced by nonresonant optical pumping with single-ring beams. Using the spectral tomography of the real-space condensate PL, we have obtained the spatial profiles of a set of quantized eigenmodes of an optical trap. We have demonstrated that although the set of available modes is similar for traps of different radii, the populations

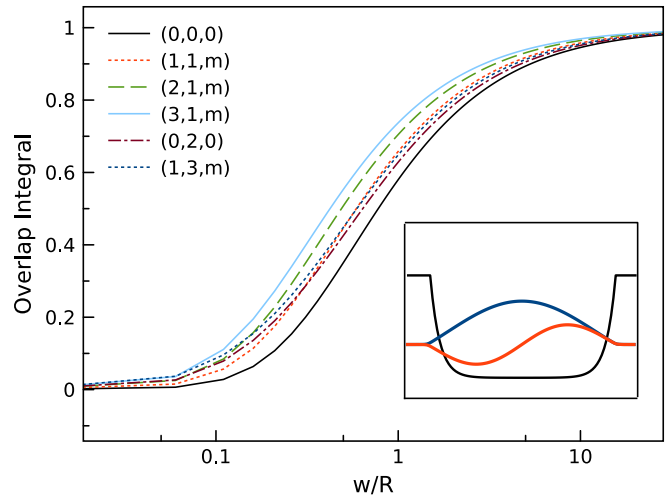

FIG. 7. The overlap integral calculated after Eq. (2) for different condensate modes as a function of the normalized exciton diffusion length w/R. The inset shows schematically the ground (blue) and the first excited (red) condensate modes in the trap potential (black).

of the modes may be strongly different, as they depend on the trapping and pumping conditions. Numerical solutions of the Schrödinger equation for a model potential enabled us to confirm that the polariton condensate states observed in the experiment represent eigenstates of an optically induced trap. The populations of the eigenmodes of the trap are determined by the balance of gain from the optical pumping and losses of polaritons. We have shown numerically that the gain governed by the overlap of the polariton wave function and the exciton reservoir is larger for the higher-energy polariton states as compared to the lowest-energy state. This explains the predominant population of excited polariton condensate modes in a trap under external pumping. The obtained results offer a method of controllable excitation of specific modes of exciton-polariton condensates in optically induced traps. The method can be further expanded to the study of exciton-polariton condensates with internal polariton currents characterized by nonzero topological charges.

ACKNOWLEDGMENTS

The experiment was carried out in the Spin Optics Laboratory at Saint-Petersburg State University (Grant No. 94030557). A.K. and P.G.S. acknowledge the support of Westlake University, Project No. 041020100118 and Program No. 2018R01002 funded by Leading Innovative and Entrepreneur Team Introduction Program of Zhejiang Province of China. A.K. acknowledges support from the Moscow Institute of Physics and Technology under the Priority 2030 Strategic Academic Leadership Program.

[1] A. Kavokin, J. Baumberg, G. Malpuech, and F. Laussy, *Microcavities*, 2nd ed., Series on Semiconductor Science and Technology (Oxford University Press, Oxford, UK, 2017).

[2] J. Kasprzak, M. Richard, S. Kundermann, A. Baas, P. Jeambrun, J. M. J. Keeling, F. M. Marchetti, M. H. Szymanska, R. Andre, J. L. Staehli, V. Savona, P. B. Littlewood, B. Deveaud, and L. S. Dang, Bose–Einstein condensation of exciton polaritons, Nature (London) **443**, 409 (2006).

[3] M. H. Anderson, J. R. Ensher, M. R. Matthews, C. E. Wieman, and E. A. Cornell, Observation of Bose-Einstein condensation in a dilute atomic vapor, Science **269**, 198 (1995).

[4] E. M. Lifshitz and L. P. Pitaevski, *Statistical Physics, Part 2*, Course of Theoretical Physics, Vol. 9 (Pergamon, New York, 1980).

[5] M. Glazov and R. Suris, Exciton condensation in a two-dimensional system with disorder, J. Exp. Theor. Phys. **126**, 833 (2018).

[6] H. Deng, G. Weihs, C. Santori, J. Bloch, and Y. Yamamoto, Condensation of semiconductor microcavity exciton polaritons, Science **298**, 199 (2002).

[7] D. Bajoni, E. Wertz, P. Senellart, A. Miard, E. Semenova, A. Lemaître, I. Sagnes, S. Bouchoule, and J. Bloch, Excitonic polaritons in semiconductor micropillars, Acta Phys. Pol., A **114**, 933 (2008).

[8] D. Bajoni, P. Senellart, E. Wertz, I. Sagnes, A. Miard, A. Lemaître, and J. Bloch, Polariton Laser Using Single Micropillar GaAs-GaAlAs Semiconductor Cavities, Phys. Rev. Lett. **100**, 047401 (2008).

[9] D. M. Myers, B. Ozden, M. Steger, E. Sedov, A. Kavokin, K. West, L. N. Pfeiffer, and D. W. Snoke, Superlinear increase of photocurrent due to stimulated scattering into a polariton condensate, Phys. Rev. B **98**, 045301 (2018).

[10] V. K. Kalevich, M. M. Afanasiev, L. K. V. Kavokin, S. I. Tsintzos, P. G. Savvidis, and A. V. Kavokin, Ring-shaped polariton lasing in pillar microcavities, J. Appl. Phys. **115**, 094304 (2014).

[11] V. A. Lukoshkin, V. K. Kalevich, M. M. Afanasiev, K. V. Kavokin, Z. Hatzopoulos, P. G. Savvidis, E. S. Sedov, and A. V. Kavokin, Persistent circular currents of exciton-polaritons in cylindrical pillar microcavities, Phys. Rev. B **97**, 195149 (2018).

[12] E. Sedov, V. Lukoshkin, V. Kalevich, Z. Hatzopoulos, P. Savvidis, and A. Kavokin, Persistent currents in half-moon polariton condensates, ACS Photonics **7**, 1163 (2020).

[13] V. Lukoshkin, E. Sedov, V. Kalevich, Z. Hatzopoulos, P. G. Savvidis, and A. Kavokin, Steady state oscillations of circular currents in concentric polariton condensates, arXiv:2210.05306.

[14] V. K. Kalevich, M. M. Afanasiev, V. A. Lukoshkin, D. D. Solnyshkov, G. Malpuech, K. V. Kavokin, S. I. Tsintzos, Z. Hatzopoulos, P. G. Savvidis, and A. V. Kavokin, Controllable structuring of exciton-polariton condensates in cylindrical pillar microcavities, Phys. Rev. B **91**, 045305 (2015).

[15] E. Sedov, V. Lukoshkin, V. Kalevich, Z. Hatzopoulos, P. G. Savvidis, and A. Kavokin, Double ring polariton condensates with polariton vortices, arXiv:2210.05300.

[16] R. I. Kaitouni, O. El Daïf, A. Baas, M. Richard, T. Paraiso, P. Lugan, T. Guillet, F. Morier-Genoud, J. D. Ganière, J. L. Staehli, V. Savona, and B. Deveaud, Engineering the spatial confinement of exciton polaritons in semiconductors, Phys. Rev. B **74**, 155311 (2006).

[17] A. S. Kuznetsov, P. L. J. Helgers, K. Biermann, and P. V. Santos, Quantum confinement of exciton-polaritons in a structured (Al,Ga)As microcavity, Phys. Rev. B **97**, 195309 (2018).

[18] B. Nelsen, R. Balili, D. W. Snoke, L. Pfeiffer, and K. West, Lasing and polariton condensation: Two distinct transitions in GaAs microcavities with stress traps, J. Appl. Phys. **105**, 122414 (2009).

[19] R. Balili, V. Hartwell, D. Snoke, L. Pfeiffer, and K. West, Bose-Einstein condensation of microcavity polaritons in a trap, Science **316**, 1007 (2007).

[20] C. Schneider, K. Winkler, M. D. Fraser, M. Kamp, Y. Yamamoto, E. A. Ostrovskaya, and S. Höfling, Exciton-polariton trapping and potential landscape engineering, Rep. Prog. Phys. **80**, 016503 (2017).

[21] A. Askitopoulos, A. V. Nalitov, E. S. Sedov, L. Pickup, E. D. Cherotchenko, Z. Hatzopoulos, P. G. Savvidis, A. V. Kavokin,

and P. G. Lagoudakis, All-optical quantum fluid spin beam splitter, Phys. Rev. B **97**, 235303 (2018).

[22] A. Askitopoulos, H. Ohadi, A. V. Kavokin, Z. Hatzopoulos, P. G. Savvidis, and P. G. Lagoudakis, Polariton condensation in an optically induced two-dimensional potential, Phys. Rev. B **88**, 041308(R) (2013).

[23] Y. C. Balas, E. S. Sedov, G. G. Paschos, Z. Hatzopoulos, H. Ohadi, A. V. Kavokin, and P. G. Savvidis, Stochastic Single-Shot Polarization Pinning of Polariton Condensate at High Temperatures, Phys. Rev. Lett. **128**, 117401 (2022).

[24] K. Orfanakis, A. F. Tzortzakakis, D. Petrosyan, P. G. Savvidis, and H. Ohadi, Ultralong temporal coherence in optically trapped exciton-polariton condensates, Phys. Rev. B **103**, 235313 (2021).

[25] R. Dall, M. D. Fraser, A. S. Desyatnikov, G. Li, S. Brodbeck, M. Kamp, C. Schneider, S. Höfling, and E. A. Ostrovskaya, Creation of Orbital Angular Momentum States with Chiral Polaritonic Lenses, Phys. Rev. Lett. **113**, 200404 (2014).

[26] J. Borat, R. Cherbunin, E. Sedov, E. Aladinskaia, A. Liubomirov, V. Litvyak, M. Petrov, X. Zhou, Z. Hatzopoulos, A. Kavokin, and P. G. Savvidis, Stochastic circular persistent currents of exciton polaritons, arXiv:2210.05299.

[27] B. Berger, D. Schmidt, X. Ma, S. Schumacher, C. Schneider, S. Höfling, and M. Aßmann, Formation dynamics of exciton-polariton vortices created by nonresonant annular pumping, Phys. Rev. B **101**, 245309 (2020).

[28] C. Antón, D. Solnyshkov, G. Tosi, M. D. Martín, Z. Hatzopoulos, G. Deligeorgis, P. G. Savvidis, G. Malpuech, and L. Viña, Ignition and formation dynamics of a polariton condensate on a semiconductor microcavity pillar, Phys. Rev. B **90**, 155311 (2014).